Paleoenvironmental reconstruction from marine core JM05-30-GC2-1, North West Svalbard Slope

Stefán Benediktsson

Jarðvísindadeild
Háskóli Íslands
2013

Paleoenvironmental reconstruction from marine core JM05-30-GC2-1, North West Svalbard Slope

Umhverfisbreytingar lesnar úr sjávarsetkjarna JM05-30-GC2-1, norðvestur af Svalbarða

Stefán Benediktsson

10 eininga ritgerð sem er hluti af
Baccalaureus Scientiarum gráðu í jarðfræði

Leiðbeinendur
Esther Ruth Guðmundsdóttir
Hreggviður Norðdahl

Jarðvísindadeild
Verkfræði- og náttúruvísindasvið
Háskóli Íslands
Reykjavík, febrúar 2013

Paleoenvironmental reconstruction from marine core JM05-30-GC2-1, North West Svalbard Slope
10 eininga ritgerð sem er hluti af *Baccalaureus Scientiarum* gráðu í Jarðfræði

Jarðvísindadeild
Verkfræði- og náttúruvísindasvið
Háskóli Íslands
Askja, Sturlugötu 7
101 Reykjavík

Sími: 525 4000

Skráningarupplýsingar:
Stefán Benediktsson, 2013, *Paleoenvironmental reconstruction from marine core JM05-30-GC2-1, North West Svalbard Slope,* BS ritgerð, Jarðvísindadeild, Háskóli Íslands, 31 bls.

Prentun: Háskólaprent
Reykjavík, janúar 2013

Yfirlýsing höfundar

Hér með lýsi ég því yfir að ritgerð þessi er samin af mér og að hún hefur hvorki að hluta né heild verið lögð fram áður til hærri prófgráðu.

_____

Stefán Benediktsson
Kt. 031088-2409
janúar 2013

Útdráttur

Rannsókn þessi miðar að því að afla upplýsinga um fornar umhverfisbreytingar noðvestur af Svalbarða. Til þess var sjávarsetkjarni JM05-30-GC2, tekinn úr norð-vestur landgrunnshlið Svalbarða (79°39N og 06°34E). Efstu 100 cm kjarnans eru skoðaðir sem taldir eru spanna síðustu 5000 ár. Aðferðirnar sem voru notaðar eru kjarnalýsing, segulviðtak, og skúfstyrkur. Tíu sýni voru rannsökuð með tilliti til vatnsmagns, kornastærðar, ís borins efnis og götunga.

Hlestu niðurstöður eru að þessi kjarni samanstendur úr leðju með einstaka fallsteinum sem gefur til kynna að setið hefur myndast í lág orku umhverfi sem verður fyrir áhrifum ísjaka og/eða hafís. Samkvæmt fyrri rannsókn er hugsanlegur aldur á botni kjarnans 5000 kvörðuð ár fyrir okkar tíma. Stærsta breytingin sem verður á setmyndun kjarnans er í efstu 5-10 cm, hugsanlegar útskýringar á því hversvegna svo gróft set finnst þarna eru gruggstraumar eða eðjustraumar og/eða aukinn hafís eða ísjakar vegna afjöklunar við lok Littlu Ísaldar.

Abstract

This study aims at reconstructing past environmental conditions northwest of Svalbard. Marine sediment core JM05-30-GC2 is used for the study. The uppermost 100 cm of the core have been investigated which is estimated to cover the past 5000 years. Multiple methods were used to reconstruct the past conditions of sedimentation and oceanography. The methods that were used are lithological logging, magnetic susceptibility, shear strength, water content measurements, ice rafted debris (IRD) count, granulometry and foraminifera analyses. Ten samples were collected from the core to measure the water content, granulometry, IRD and foraminifera.

The main findings are that this core consists of massive mud with occasional dropstones which indicates low energy deep water marine environment that is affected by ice rafted debris from icebergs and/or sea ice. A speculative age of the bottom of the core is given as 5000 calibrated years BP. The biggest change in sedimentation is at the top 5-10 cm of the core, possible explanations for the coarse grains at the top are slope failures and turbidity flows and/or glacial calving during deglaciation after the Little Ice Age.

Table of contents

List of Figures

List of Tables

Acknowledgements

I want to thank the University Center in Svalbard for two awesome semesters. I want to thank my Svalbard traveling companions Gauti and Hrafnhildur, because without them I would have never gone to Svalbard.

I want to thank Oliver, Chloé and Alice for all the help with this project.

I want to thank Esther Ruth Guðmundsdóttir and Hreggviður Norðdahl for all the advices and assistance.

I want to thank my family for all the support.

1 Introduction

Global climate change has become a big topic in the past years. Studies have shown that the Arctic climate is showing signs of rapid change. The Arctic Ocean ice cover is decreasing on average 2 – 3% per decade (Slubowska et al., 2005). Scientists believe that the cause of this rapid warming is human-released greenhouse gases. To understand the changes in the climate, paleoclimate and paleoceanography must be studied. One of the reasons we want to be able to reconstruct the past is to be able to predict the future.

Sometimes it is forgotten in the discussion that the global climate change is not only affecting the air temperature around the world but also the temperature and chemistry of the ocean. But these systems are of course connected; changes that happen above sea level have effects in the sea and the other way around. Ever since the 1990s scientists have recognized that dramatic changes were happening in the Arctic. The permafrost was thawing, reduced sea ice cover, increase in precipitation and freshwater river discharge, increased Atlantic water inflow into the Arctic. According to climate model simulations the Arctic Ocean may become ice-free during summer before the end of this century. This can cause reduced albedo effect and therefore thawing of permafrost which may release greenhouse gases into the atmosphere which may then increase the warming even more. Freshwater from river runoff and glacier melt-water to the Arctic Ocean raise global sea level and may possibly slow down the global thermohaline circulation. It is evident that changes in the Arctic Ocean could cause a major unbalance in the global climate and environment (Stein, 2008).

The aim of this study is to use multiple methods to reconstruct past conditions of sedimentation and oceanography at the NW Svalbard slope. The methods that were used on the marine sediment core JM05-30-GC2-1 are Lithological logging, magnetic susceptibility, shear strength, water content, granulometry, ice rafted debris count and foraminifera analyses.

The core was taken along the north-western Svalbard slope 79°39N and 06°34E, at around 1073 meter water depth, with the multipurpose research vessel Jan Mayen in May 2005 (Jessen et al., 2010). The University of Tromsø is the owner of the vessel and other users of the vessel are Institute of Marine Research, Bergen and the University Center in Svalbard.

2 Physical setting

2.1 Geographical setting

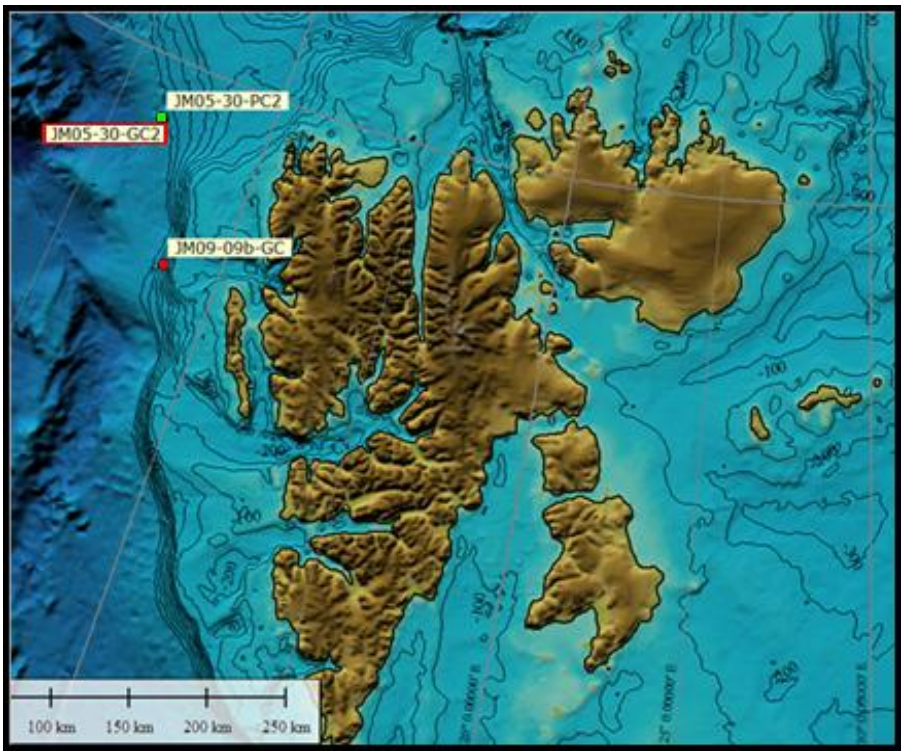

Figure 2.1 Location of the core on the north-western Svalbad slope. The core site is marked with a green dot (source: Riko Noormets)

The Svalbard archipelago (figure 2.1) is located in the Arctic Ocean between 76°and 81°N. The total land area is 62.160 km^2. The main islands are Spitsbergen Nordaustlandet, Barentsoya, Edgeoya, Kong Karls Land, Prins Karls Forland and Bjornoya. The largest islands are Spitsbergen and Nordaustlandet, they are separated by a 170 km long strait, named the Hinlopen Strait. Around 60% of Svalbard is covered by glaciers at present. Although Svalbard is located in the high Arctic, the climate is relatively mild. Mean annual Temperature is around -6°C, when other regions at similar latitude are compared for example East Greenland has mean annual temperature around -16°C (Ingólfsson & Hormes, 2009). The key factor behind this difference is the relatively warm and saline West Spitsbergen Current (WSC) which flows to the western and northern parts of Svalbard (Slubowska et al., 2007)

2.2 Sedimentary environment

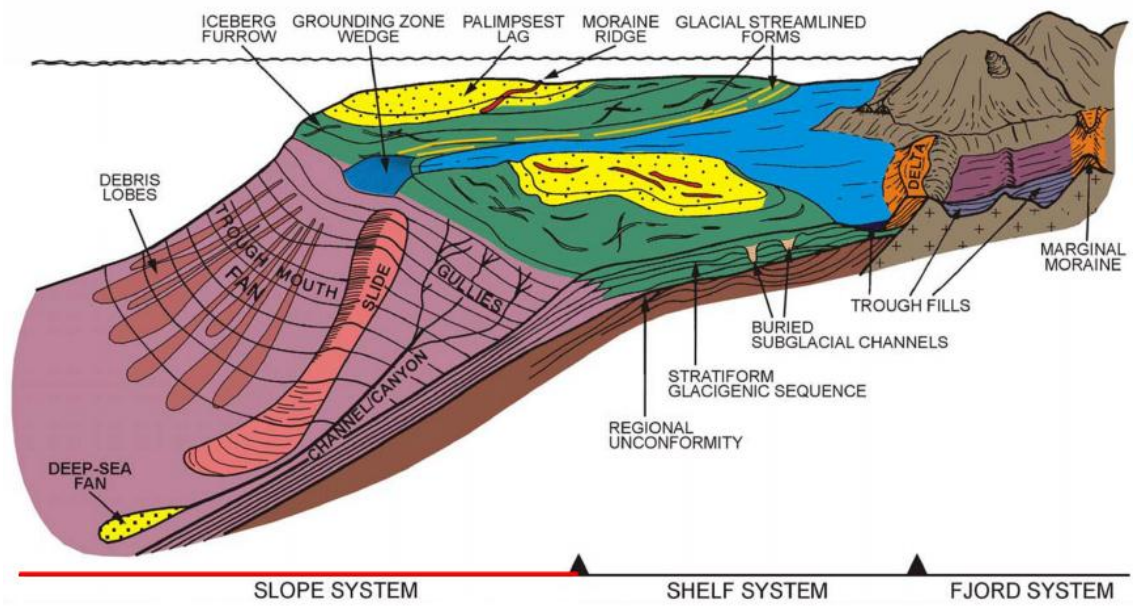

Figure 2.2 A cartoon of a slope system similar to the north-western Svalbard slope. (source: Benn & Evans, 2010)

As mentioned previously the core was taken from the north-western slope (figure 2.2) of Svalbard. The western Svalbard slope mostly consists of late Pliocene to Quaternary sediments, which are deposited in glaciological trough-mouth fans. During full glacial conditions, thick mass transport and deposition of sediments occur on the Through-Mouth Fans. In the inter-fan areas thin mass transport deposits are also found (Jessen et al., 2010). During glacial conditions increase in ice rafted debris (IRD) is expected and finer mud and silts are expected during interglacial (Stein, 2008). Because the core is taken from a slope, there is a possibility that it has been reworked by slope failures and turbidity flows.

2.3 Oceanography

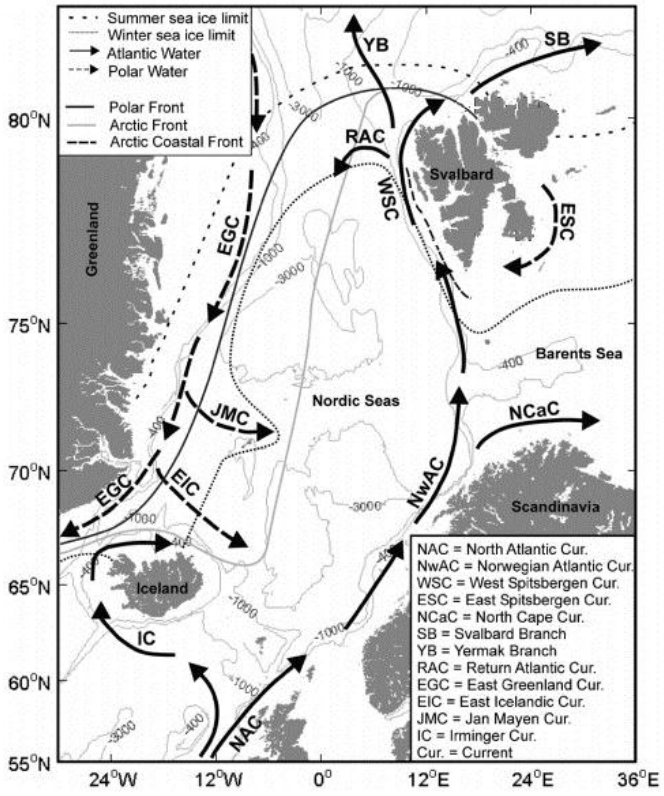

Figure 2.3 Map with major surface currents and winter-summer sea ice limits (source: modified Slubowska 2007).

The Arctic Ocean is the smallest, shallowest and has the lowest salinity on average of the five major oceanic divisions. The opening of the Fram strait as a deep water passage around 18.5 million years ago connected the Arctic Ocean to the World Ocean. Fram strait is the only deep strait (2600m) located between Svalbard and Greenland (figure 2.3). The Western Spitsbergen Current (WSC) and the East Greenland Current (EGC) meet in the Fram strait. The Western Spitsbergen Current transports Atlantic water, Atlantic Intermediate water and Norwegian Sea Deep Water. This transport is thought to be the main source of warm and saline water to the Arctic (Stein, 2008). In the Fram Strait the WSC sinks down and forms the Atlantic Layer which has temperature of 0 – 2°C and salinity of 34.7 – 35 ppt (Slubowska et al., 2005). Most of the Atlantic Water recirculates in the Fram Strait back south below the cold East Greenland Current (Jessen et al., 2010). Circulation like this is an important driver of global ocean circulation. The East Greenland Current flows southward along the east coast of Greenland. It is the main transporter of ice from the Arctic Ocean. The water masses it transports are Polar Water, recirculating Atlantic Water and Deep Water. The Polar Water has depth from surface to around 150 meters. Temperature range from 0 – 1.7°C and salinity goes from 30 ppt at surface to 34 ppt at 150 meters depth. The low salinity of the surface layer is due to sea ice melting and freshwater river runoff. Below the Polar Water is the Atlantic Water and it extends down to 1000 meters depth. Temperature is above 0°C and salinity is 34 – 35 ppt (Schlichtholz & Houssais, 1999). Below 1000 meters depth comes Deep Water with relatively constant temperature below 0°C and salinity around 35 ppt (Aagaard & Coachman, 1968).

3 Previous study

A study previously done by Jessen et al. (2010) collected this core and many others located on the West Svalbard Slope. A calibration curve of stacked depth against ^{14}C was made from chronology of cores. According to this calibration curve the bottom of the core JM05-30-GC2-1 is approximately 5000 calibrated years BP (figure 3.1).

The study shows that between 10.100 and 7600 ±100 years BP. IRD was low which implies that very few icebergs were released to the ocean because of the northward passing of the Polar front and first strong inflow of Atlantic surface Water. But then the Atlantic water cooled and land ice started to re-advance and ice rafting increased again (Jessen et al., 2010).

Concentration of IRD in cores JM03-373PC2 and JM04-025PC gradually increase from 5700 to 2600 cal years BP which indicate increase in icebergs and/or sea ice southwest of Svalbard and the Barents Sea (figure 3.2) (Jessen et al., 2010). Both these cores were taken from the south west Svalbard slope.

Svendsen and Mangerud (1997) studied the Holocene glacial and climate variations on Spitsbergen and concluded that the glaciers started to advance from 5200 cal years BP and reached their full extent during the Little Ice Age (Jessen et al., 2010).

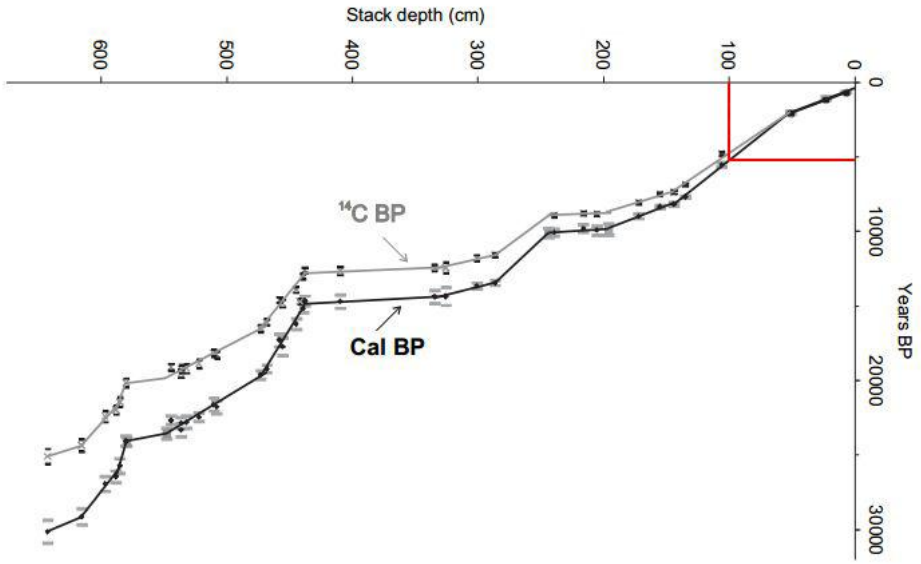

Figure 3.1 ^{14}C and calibrated age models for the stacked MS-chronology. Dates are presented with ±2s uncertainties (source: Jessen et al., 2010 page 1307). Bottom of the core is shown by the red line.

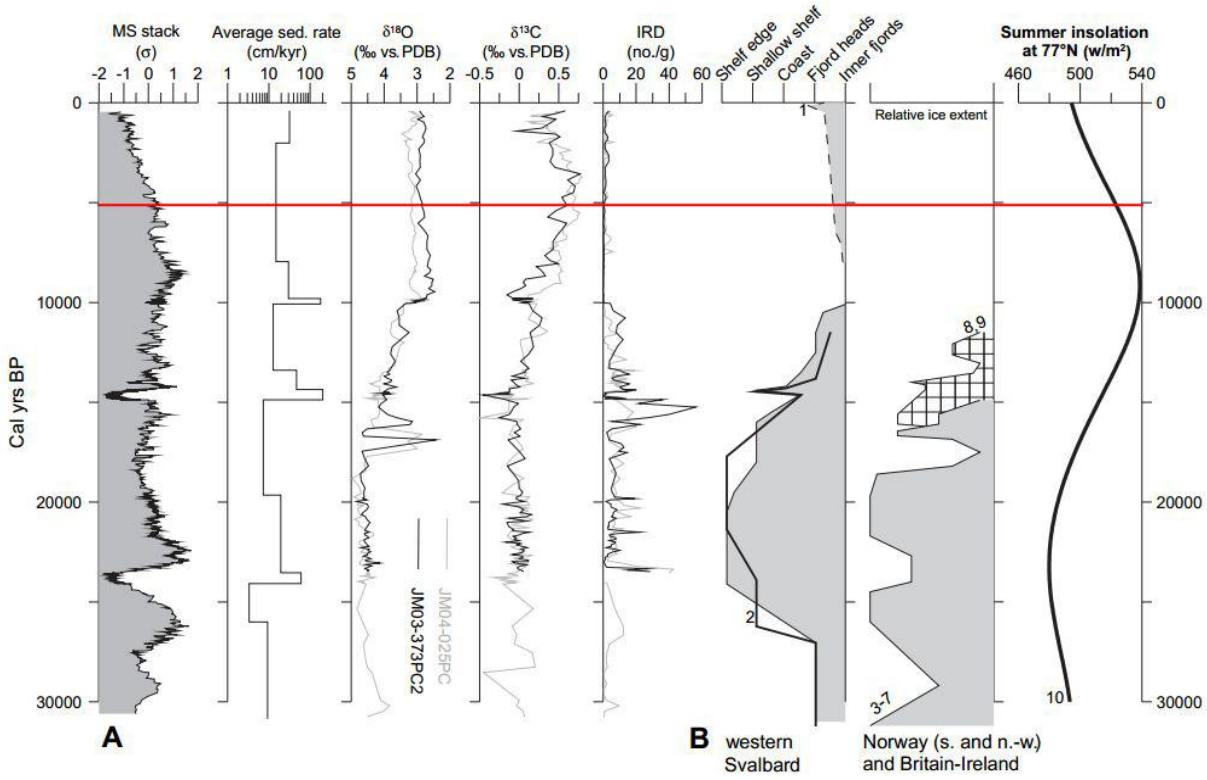

Figure 3.2 A: Record made by Jessen et al. (2010) from two cores taken on the western Svalbard slope, core JM03-373PC2 (76°24 N 1485m water depth) and JM04-025PC (77°40 N 1880 m water depth). B: Glaciation curve for western Svalbard, southern and western Norway, Britain and Ireland. Summer insolation for 77°N from June 21 to July 20. (source: Jessen et al., 2010 page 1308)

4 Foraminifera

Foraminifera are single celled protozoa ranging from Early Cambrian to present. They have soft tissue enclosed in a shell. The shell can be composed of secreted tectin which is an organic matter or the shell may be composed of secreted minerals which are calcite, aragonite, and silica or agglutinated particles. The shell can have single or multiple chambers which are connected by openings or foramina which the group takes its name from. Most of the species live on or within the seafloor and are called benthic. The others float at various depths in the water column and are called planktonic. Around 30 percent of the ocean floor is covered with dead foraminiferan empty shells which are called foraminiferal ooze (Rogers, 2011). Foraminiferas can be used to reconstruct past environmental conditions (Hald & Korsun, 1997). By looking at how present foraminifer species live in a certain type of environment, than past foraminifer must have lived in a similar environment. Examining stable isotope ratios of oxygen and carbon in the shells can also be used to reconstruct past environmental conditions (Zachos et al., 2001).

The major environmental factors that affect planktonic foraminifera in general are surface-water temperature, surface-water salinity, food supply, and predation. But in the Arctic Ocean the diversity is largely controlled by permanent sea-ice cover, the high freshwater discharge, and nutrient and food availability (Volkmann, 2000).

Compared to the planktonic species the benthic species has much higher species richness. The major environmental factor that affect benthic foraminifera in the Arctic Ocean are not fully understood but some are known for certain, changes in water masses, surface-water productivity, and/or sea ice conditions (Wollenburg et al., 2004).

4.1 Foraminifera in core JM05-30-GC2-1

The most common foraminifera's found in the core JM05-30-GC2-1 were *Islandiella helenae* and *Neogloboquadrina pachyderma*. Other foraminiferas found in the core are *Cassidulina reniforme, Elphidium hallandense, Stainforthia loeblichi* and *E. excavatum f. clabata*.

Planktonic:

Neogloboquadrina pachyderma: Is the most common species of planktonic foraminifers in the Arctic Ocean (Volkmann, 2000). It favors open sea condition, avoids low salinity, thrives in Atlantic derived masses, and shows highest abundances during interglacials (Stein, 2008). *Islandiella helenae* and *N. pachyderma* together indicate a deep water environment (Hald and Korsun, 1997).

Benthic:

Islandiella helenae: Is a high arctic open-ocean species which requires stable salinity. Indicates increased sea ice cover, glacier-distal environment and proximity of the sea ice edge (Kubischta et al., 2010).

Stainforthia Loeblichi: Thrives in cold waters around 0°C and indicates seasonal ice cover in the area (Steinsund et al., 1994).

Elphidium hallandense: Is a high arctic species indicating shallow water and/or brackish water condition, brackish water is in-between fresh water and saline water with salinity of 0.5 – 30 ppt and may result from seawater and freshwater mixing. Prefers silty and sandy seafloor (Hansen & Knudsen 1995).

Elphidium excavatum f. clavata: This foraminifer habitat is near a glacier terminal and the terminal of the sea ice extent (Hald & Korsun, 1997).

Cassidulina reniforme: This foraminifer habitat is in glacio-marine environment (Hald & Korsun, 1997).

5 Methods

5.1 Gravity corer

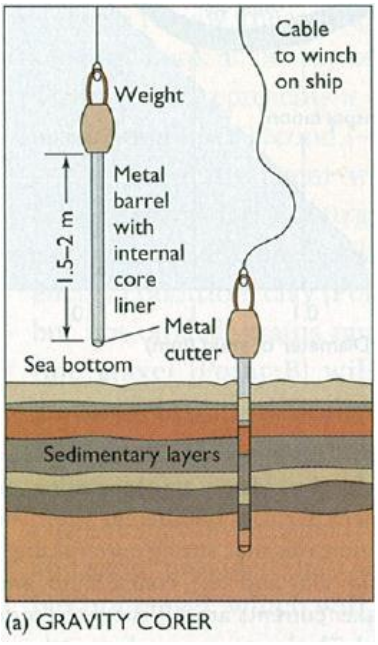

Figure 5.1 Cartoon of a gravity corer (Paul R. Pinet, 2008 page 95)

The core JM-05-30-GC2-1 was retrieved in 2005 by the research vessel Jan Mayen using a gravity corer method. It is a simple coring method, a tube with a plastic liner and a heavy weight at the top is lower down until it hits the see floor and drives the tube into the sediment (figure 5.1). The gravity corer is then hauled back up to the ship and is measured and cut into 1 meter sections and stored in a dark cool place. Gravity corers can take cores of between 1 and 8 meters long. The amount of core sample is also limited to sediment properties.

5.2 Lithological Logging

The split core was first measured from bottom to top and was measured around 1 meter. Using a microscope slide the surface of the core was cleaned by scraping horizontally to better reveal color changes and boundaries. The sediment properties of the core were described such as color, structure, grain size, drop stones and shell fragments. Pictures were taken of the core.

5.3 Magnetic Susceptibility

The matter that normally controls the magnetic susceptibility is variation in amount of ferromagnetic matter, that is mainly magnetite, pyrrhotite, olivine, biotite, pyrite and iron-oxide-stained rock and mineral fragments. Matter that gives low readings in magnetic

susceptibility is biogenic material for example calcite and silica, and quartz and feldspar (Rothwell & Rack, 2006). Therefore magnetic susceptibility can be used to find out changes in composition and source areas of terrigenous sediments. Water has an effect on magnetic susceptibility and therefore much water can lower the signal (Stein, 2008). Magnetic susceptibility has been used to detect ice rafted debris (Pirrung et al., 2002).

A Bartington MS2E1 sensor was used to measure magnetic susceptibility. The range was 0.1, drift limit was five and the interval (resolution) was two cm. The Barington M2E1 is a handheld device and is very sensitive so it is not recommended to be wearing or having any metallic things around the device when it is measuring. The measuring was done twice and showed a very similar graph so the two measurements were merged together and thus show an average of two measurements.

5.4 Shear Strength

Shear strength describes the strength of a material. Varying shear strengths represent varying lithologies. A GeoNor fall-cone penetrometer was used, along with two types of 30° cones a 400g and a 100g cone. The cone was relished onto the core and penetrated it; the depth of the penetration was recorded for the left and right side of the core at five cm intervals. The average penetration was calculated and then converted to kilopascals using a calibration table.

5.5 Water Content

Ten samples were taken from the core at the depths of 2cm, 12cm, 22cm, 32cm, 42cm, 52cm, 62cm, 72cm, 83cm and 95cm. The samples were extracted with a syringe to get a sample size of 8ml but because the core was a little bent/pressed down, only five to six ml made it into the syringe. The samples from the syringe were put in cups and weighted. The cups were then dried in a 60°C heater for 24 hours. The amount of water was calculated as a percentage of the total weight with the following formula (Eq. 5.5).

$$[Eq.\,5.5] \quad Wc = \left(\frac{m_{wet} - m_{dry}}{m_{wet}}\right) * 100$$

Where:

Wc = Water content percentage

m_{wet} = Wet weight of the sample

m_{dry} = Dry weight of the sample

5.6 Granulometry

The samples that were collected for the water content measurements were then sieved using three size fractions, 63µm, 100µm and 1000µm. Grain sizes percentages where calculated as a part of the total weight of the sample and give the percentage of <63µm (mud), 63-100µm (fines and sands), 100-1000µm (forams and IRD) and >1000µm.

$$[Eq.5.6] \quad Gs = \left(\frac{100}{S-P}\right) * F - P$$

Where:

Gs = Grain size percentage

S = Total dry sample weight, including the sieve

P = Weight of empty sieve

F = Sieved fraction weight, including the sieve

5.7 Ice Rafted Debris Count

Ice rafted debris (IRD) can be an indicator of icebergs and/or sea ice has traveled over and deposited sediments transported from their source area in some cases thousands of kilometers (Rafferty, 2011).

Grains bigger than >1000µm IRD were counted underneath a microscope. To count the number of ice rafted debris per gram of sample, up to 100 were counted per sample, which was then applied to the entire dry weight using equation (Eq. 5.7). All the samples did not meet the minimum count of 100. Split coefficient was 1 in all calculations.

$$[Eq.5.7] \quad IRDg = \left(\frac{45 * 1g}{N * D}\right) * I * S$$

Where:

IRDg = Number of IRD grains per gram of sample

N = Number of squares from microscope tray counted

D = Dry weight of sample

I = Number of IRD grains counted in sample

S = Split coefficient (0 split = 1, 1 split = 2, 2 split = 4 etc)

5.8 Microfossils

Foraminifera in the 100 µm size fraction was analysed and counted under a microscope using a microscope tray. To count the number of foraminifers per gram of sample, up to 100 were counted per sample, which was then applied to the entire dry weight using equation (Eq. 5.8). Samples that did not meet the minimum count of 100 were samples 1, 2, 3, 4, 5 and 7. Split coefficient was 1 in all calculations.

$$[Eq.\,5.8] \qquad Fg = \left(\frac{45 * 1g}{N * D}\right) * F * S$$

Where:

Fg = Number of forams per gram of sample

N = Number of squares from microscope tray counted

D = Dry weight of sample

F = Number of forams counted

S = Split coefficient (0 split = 1, 1 split = 2, 2 split = 4 etc.)

6 Results

6.1 Lithological Log

Results from the lithological logging are shown in figure 6.1.

0 – 10 cm: There is sand at the top but it is fining downwards (figure 6.1 photo nr. 1). Granulometry confirms this and shows there is less mud in the top 10 cm. There was also an organism that looked like a tube around five cm depth but it has not been analysed to species.

10 – 100 cm: This interval of the core consists of massive mud with occasional dropstones and shell fragments. One dropstone was found at 19 cm depth. Multiple dropstones were found from 36 to 43 cm depth (figure 6.1 photo nr. 2). Shell fragment was found when sieving a sample from 42 cm depth.

Around 46 to 53 cm depth a color change is observed from dark gray to light gray (figure 6.1 photo nr. 3). A shell fragment was found around 58 cm depth. There are red lines at 54 to 62 cm depth that could be diatoms (figure 6.1 photo nr. 3).

Visible dropstones are observed in the core around 84 cm depth. The sediments are a little bit darker in color from 82 to 85 cm depth. The grain size shows it is coarser at this interval. Another shell fragment was found at 88 cm depth (figure 6.1 photo nr. 4).

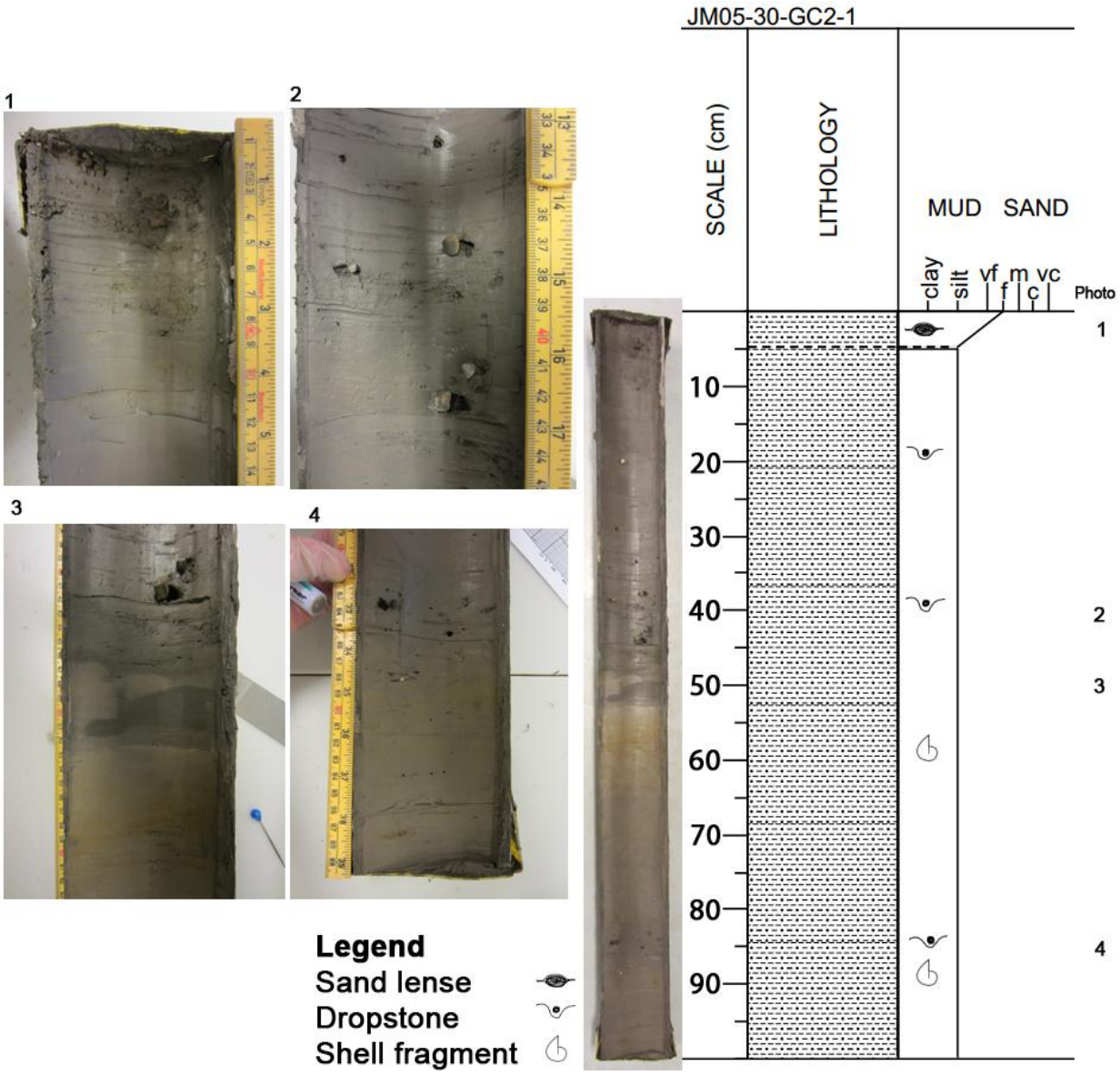

Figure 6.1 Lithological log and pictures of the core. Photo nr. 1 shows the top 14 cm of the core. Photo nr. 2 shows intervals of dropstones that were visible on the surface of the core. Photo nr. 3 shows dropstones at 43 cm, a color change from dark gray to light gray and diatoms at the bottom of the picture. Photo nr. 4 shows dropstones at 84 cm and a shell fragment at 88 cm depth.

6.2 Magnetic Susceptibility

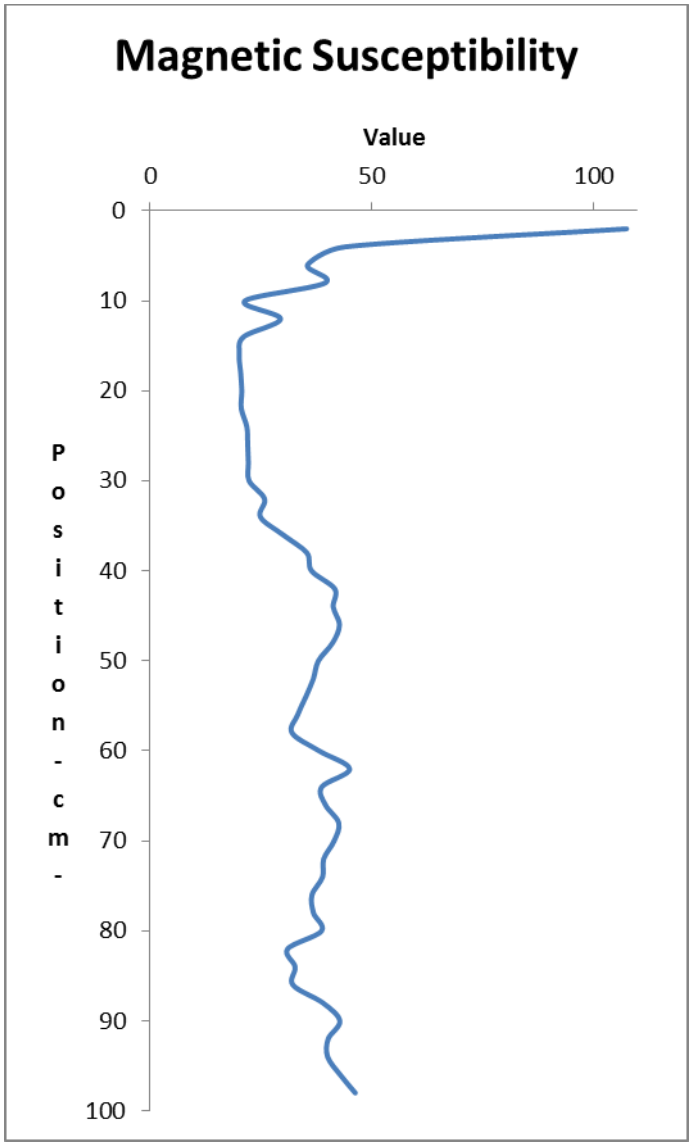

Figure 6.2 The graph shows variations in magnetic susceptibility in core JM05-30-GC2

Results from the mangetic susceptibility (MS) are shown in figure 6.2. Magnetic susceptibility starts with a major peak around 2 cm depth but decreases rapidly. Peaks are observed at 5 cm. 8 cm and 13 cm and a low is at 10 cm depth. The MS record is stable around a value of around 15-30 cm than gradually starts to climb from 32 cm to 45 cm depth than gradually decreases to 58 cm depth. Between 64 to 80 cm depth the MS is relatively stable but an increase is noticeable at 62 cm depth. Peaks are observed at 90 cm and 98 cm depths. All in all The MS (SI) varies throughout the whole core but never goes much over 40 (except in the first 5 cm) and never goes much under 20 in value.

6.3 Shear Strength

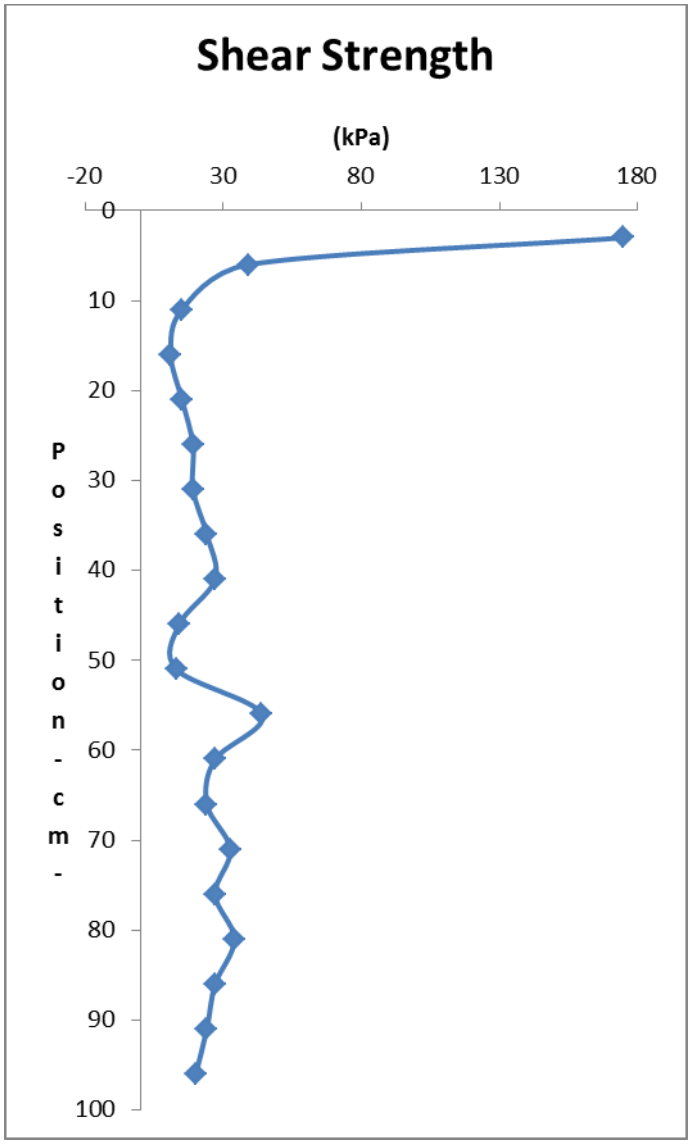

Figure 6.3 The graph shows variations shear strength in core JM05-30-GC2

Results from the shear strength are shown in figure 6.3. In the top of the core the shear strength peaks around 3 cm depth but decreases quickly at 10 cm depth. Shear strength gradually increases from 15 cm to 45 cm depth than takes a dip down at 52 cm depth but swings back up and peaks at 55 cm depth. It varies from 60 cm to 80 cm depth than gradually decreases to the end of the core. Over-all the strength of the core never goes much over 40 kPa (except in the first 5 cm) and never goes much under 10 kPa.

6.4 Water Content

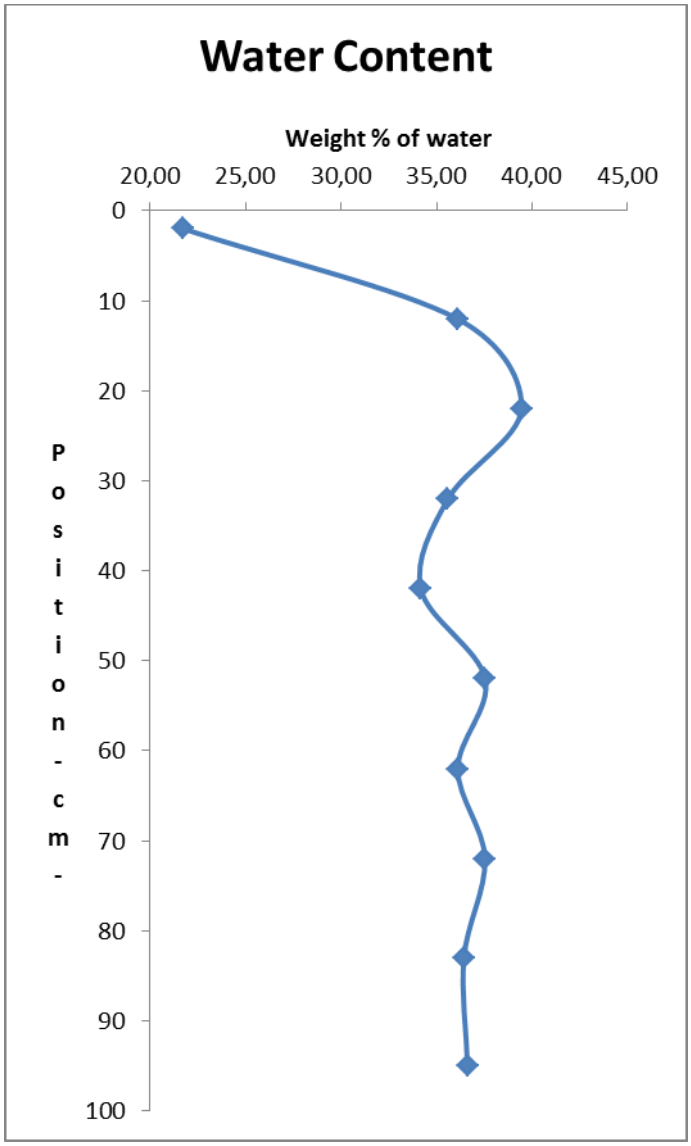

Figure 6.4 The graph shows variations in water content in core JM05-30-GC2

Results from the water content are shown in figure 6.4. Water content is lowest in the top of the core but increases and peaks at 22cm depth than gradually decrees to 42 cm depth than increases and peaks at 52 cm depth. Then stays relatively stable from 52 cm depth to the bottom of the core never deviating much from 35% water content. All in all the water content of the core never goes much over 40 % and under 34% except in the first 10 cm.

6.5 Granulometry

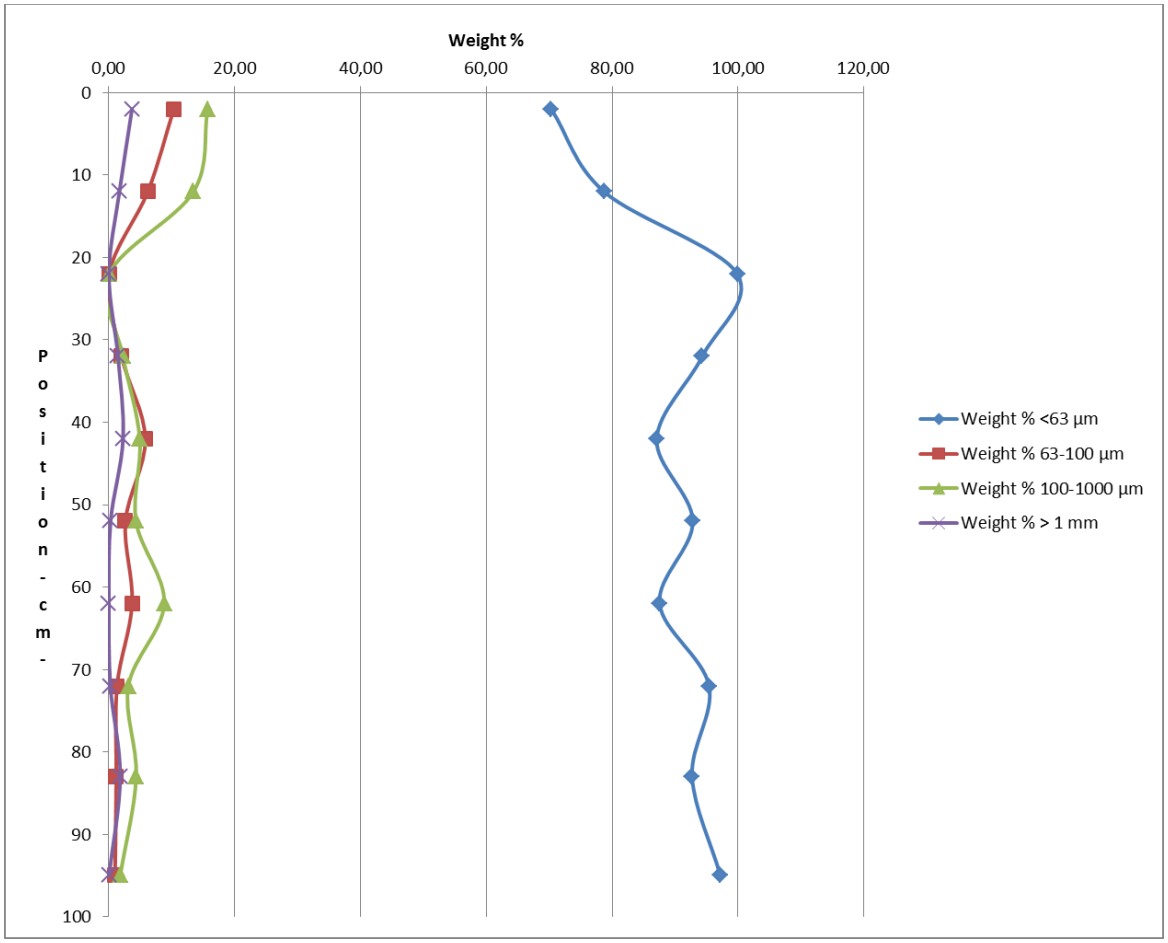

Figure 6.5 The graph shows variations in granulometry in core JM05-30-GC2

Results from the granulometry are shown in figure 6.5. The lowest amount of fine material (<63 µm) is in the top of the core. The sediments gradually become finer grained from 2 cm to 22 cm depth to fine grained with weight % of <63 µm at almost 100%. Between 22 cm to 42 cm depths the sediments gradually become coarser, then gets finer again at 52 cm. At 62 cm depth the weight % of 100 – 1000 µm increases. The grain size is relatively stable from 72 cm depth to the bottom. From 22 cm depth to the bottom of the core the weight % of <63 µm never goes below 80%.

6.6 IRD Count

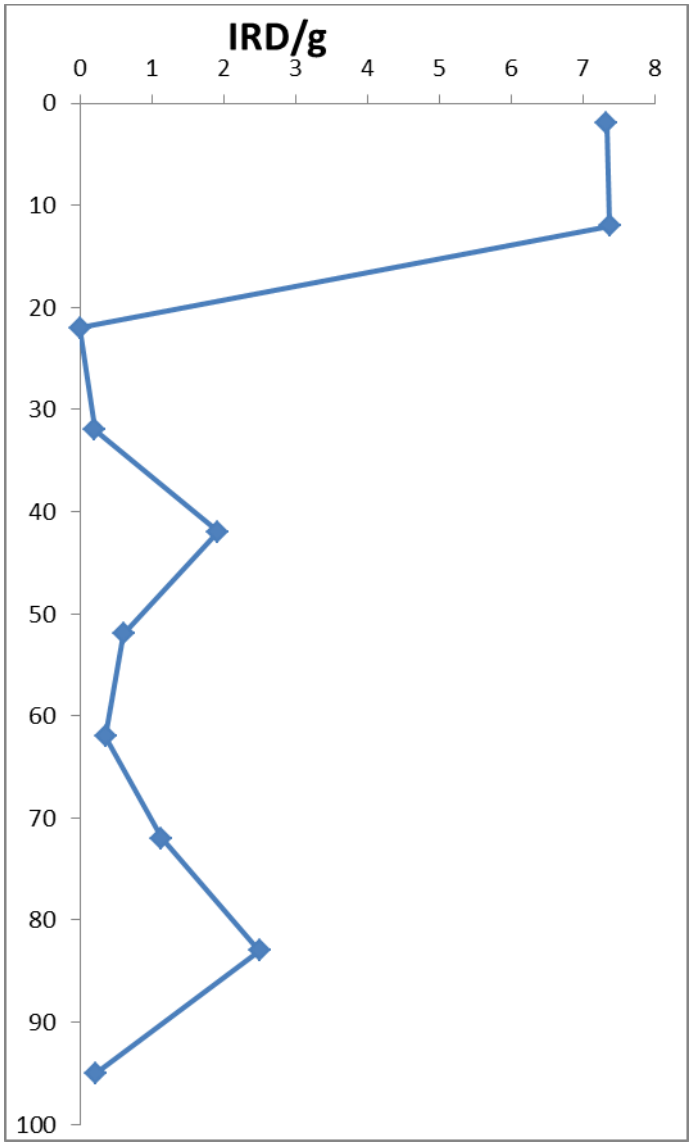

Figure 6.6 The graph shows variations in IRD/g in core JM05-30-GC2

Results from the ice rafted debris (IRD) analyses are shown in figure 6.6. Noticeably highest amount of IRD per gram is in the upper 12 cm of the core following with a sharp decline to 22 cm depth with no IRD bigger than >1 mm found. Amount of IRD stays low but peaks up at 42 cm and 83 cm depths. Total amount of IRD grains counted is 105 and ranged from 37 to 0. Only bigger than >1 mm IRD was counted.

6.7 Microfossils

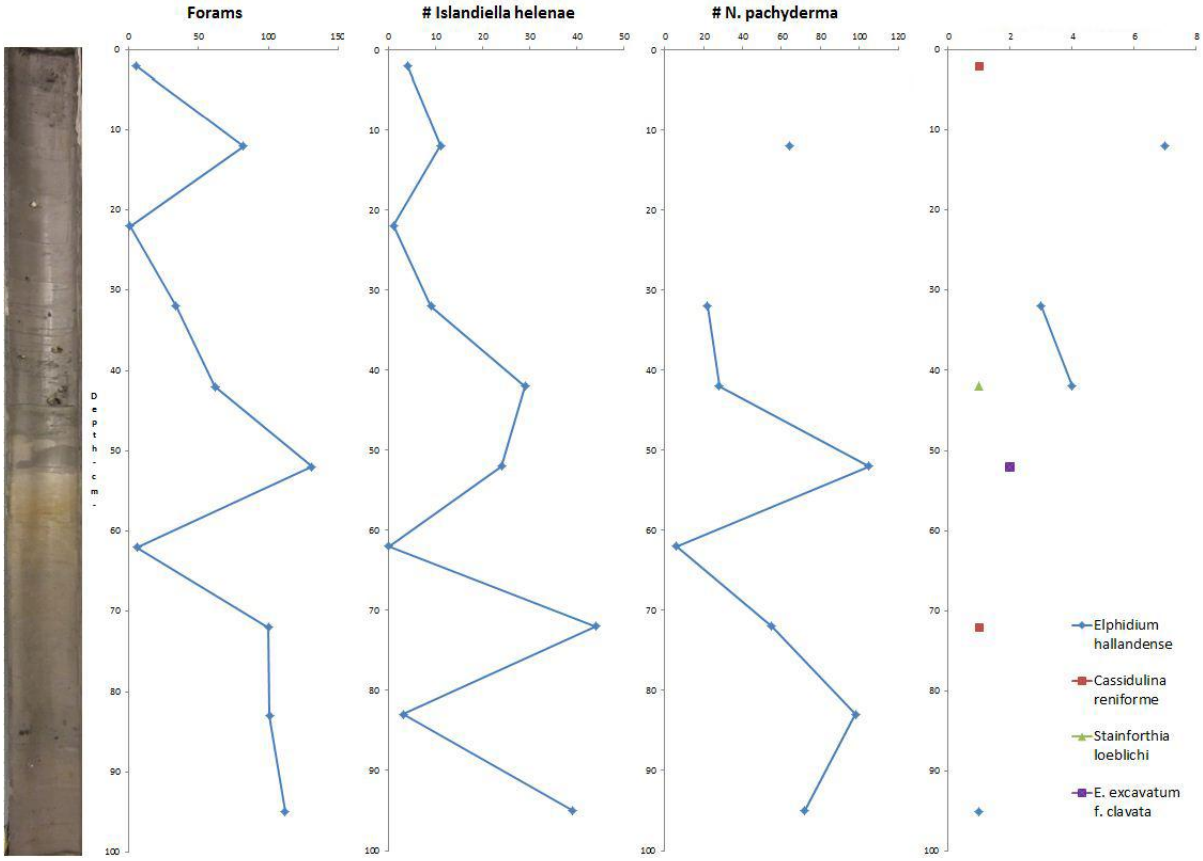

Figure 6.7 The graphs show variation in foraminifera species in core JM05-30-GC2

Results from the foraminifera count are shown in figure 6.7. Number of foraminifera varied a lot throughout the core ranging from 131 to 1. A peak at 12 cm depth is observed with a total collapse at 22 cm depth, steadily rises to 52 cm but drops at 62 cm then rises again and stays relatively stable until the bottom of the core sample.

6.8 Composite log

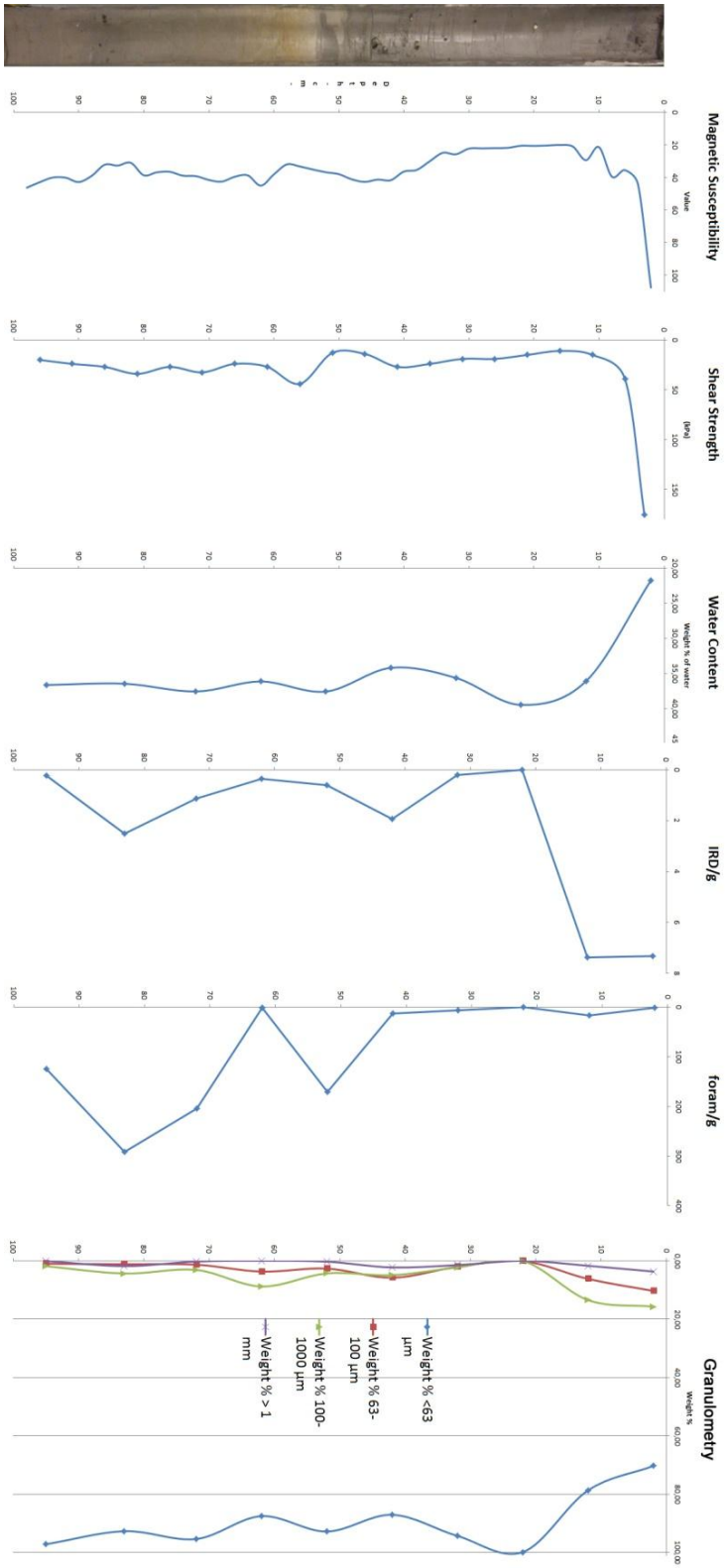

Figure 6.8 Shows a composite log of core JM05-30-GC2.

The composite log (figure 6.8) showing photograph of the core, magnetic susceptibility, shear strength, water content, IRD/g, foram/g and granulometry.

7 Discussion

The investigation on core JM05-30-GC2-1 shows changes in the environmental condition in the area for the approximately past 5000 calibrated years BP. It has to be kept in mind though that this age is speculative. The core consists of massive mud which indicates low energy deep water marine environment with intervals of ice rafted debris (IRD) and dropstones.

Magnetic susceptibility has been used to detect ice rafted debris (Pirrung et al., 2002). Correlation can be seen between magnetic susceptibility, IRD and grain size. Generally an increase in magnetic susceptibility is observed with increase in IRD rises and at intervals with coarser sediments in the core. Water content and MS also show a correlation, when water content is high the MS value decreases. The MS should therefore be able to indicate changes in sedimentation environment but it fails to show accurate correlation with other measurements.

Undrained shear strength is dependent on lithology and water content. Ideally the shear strength should be measured right away when the core is opened before any water has a chance to escape. Six years are since the collection of the core, therefore the shear strength results might not be accurate. Normal consolidation behavior should make the shear strength increase down the core (Jakobsson et al., 2001). Boundaries can be indicated by a distinct change in shear strength (Matthiessen et al., 2010).

The shear strength profile shows a correlation between strength and coarser grained sediments in the core. It can therefore be said that larger grain size yields higher shear strength. The profile shows a distinct change from the top of the core to approximately 10 cm depth, indicating change in sedimentation. Below 10 cm depth there is not much variability in the profile, indicating that the sedimentation is continuous.

Water content is very low in the top most part of the core and then increases and is very similar throughout the core. As previously mentioned the core is six years old and a lot of water has escaped in that time. Correlation can be seen between granulometry and water content. Water escapes more easily through coarse grained sediments than fine grained. Therefore there is more water content in the fine grained parts of the core.

Granulometry and IRD show clear correlation, when IRD increases the weight % of <63µm decreases. Granulometry can therefore be used to identify ice rafted debris in the core. According to the granulometry most of the core is composed of mud with grain size smaller than 63µm, which indicates a very low energy depositional environment (Benn & Evans, 2010). Coarsest sediments are found in the top 12 cm of the core indecently were the number of IRD is highest. The core is taken at a 1073 meter water depth, the depositional environment should be very low energy and it is interesting to see such coarse grains there. As previously mentioned the core is taken from a slope, thus it is possible that the top 10 cm have been affected by some kind of slope failure or turbidity flow. No clear indication can be seen though that it has been affected by slope failures or turbidity flows.

One other possibility is that the coarser grains are ice rafted debris (IRD) formed in a surge of sea ice and/or icebergs. Ice rafted debris can be used to identify glacial advance as well as deglaciation when glacial calving increases (Slubowska et al., 2005). The IRD was not studied in detail but most of them were sandstone and occasionally some granite. Large (around 5 – 20 mm) IRD/dropstones were visible on the surface of the core at depths of 19 cm, 36-43 cm and 84 cm. IRD rises at those depths except for at 19 cm depth the core is very fine grained. That indicates that even though the core is fine grained it is still being affected by ice rafted debris. Perhaps the coarse grained IRD interval at the top of the core is connected to deglaciation events after the Little Ice Age, a cold period spanning 1350-1850 AD (Dowdeswell, 1995).

Foraminifers, both planktonic and benthic, can be used as an indicator of past conditions because of their high sensitivity to environmental change (Hald & Korsun, 1997). The only planktonic foraminifer that was found in the core is *Neogloboquadrina pachyderma;* this foraminifer favors open sea condition, avoids low salinity, thriving in Atlantic derived masses, and shows highest abundances during interglacials (Stein, 2008). Therefore where this species occurs in the core, Atlantic water masses are dominating with interglacial conditions in the Arctic. *Neogloboquadrina pachyderma* was found in every sample, except for samples from 2 cm and 22 cm depths.

The most common benthic species identified at all depths in the core is *Islandiella helenae*, which is a high arctic open-ocean species, which requires stable salinity. It indicates increased sea ice cover, glacier-distal environment and proximity of the sea ice edge (Kubischta et al., 2010). *Islandiella helenae* and *N. pachyderma* together indicate a deep water environment (Hald and Korsun, 1997). Other species were found in the core at various depths but they were not consistent throughout the core. They all indicate glacio-marine environment.

The amount of foraminifera varies throughout the core. In the upper half of the core the number of foraminifera decreases drastically compared to the lower half. The reasons might be changes in water masses, surface-water productivity, and/or sea ice conditions (Wollenburg et al., 2004).

A change in color, from dark gray to light gray can be seen in the core around 55 cm depth (figure 6.1 photo nr. 3). There are no visible changes in the grain size, MS, shear strength or water content. The only thing that shows a change is the forams/g. It goes up around 52 cm depth but then again goes down around 62 cm depth and grain size increases. Forams/g increase again around 72 cm depth. There is no clear change in the sediments that can explain the color change. But below the color change at 53-64 cm depth there are red lines that could be diatoms. Diatoms provide a strong indication of changes in salinity associated with basin isolation (Kjemperud, 1986). Diatoms do not occur under extensive sea ice cover (Koc et al., 2002). Therefore the change in color might have something to do with change in salinity. Change in salinity would probably be connected to change in inflow of Atlantic surface Water. The diatoms indicate also that this area was not under extensive sea ice cover at that time.

When this study and previous study made by Jessen et al. (2010) (figure 3.1 and 3.2) are compared there can be seen some correlation in IRD but it is hard to pinpoint the exact place in the core where it happens, but show similar variations in the IRD profile. In both studies IRD never exceeds 10/g which indicates that ice rafting, in the time period of the last 5000 calibrated years BP, has been low compared to the glacial period and the deglaciation 30.000-10.000 calibrated years BP (Jessen et al., 2010).

8 Conclusion

The investigation of core JM05-30-GC2-1 shows that the sediments were formed in a low energy environment that is affected by icebergs and/or sea ice.

Comparison of the MS record in core JM05-30-GC2-1 to previous studies in the area suggest the investigated interval spans 5000 calibrated years BP. However this is speculative.

Possible explanations for coarse grains and peak in IRD in the top of the core are; slope failures and turbidity flows and/or glacial calving increase during deglaciation after the Little Ice Age.

Foraminifera and IRD indicate that this area was influenced by sea ice and was close to glaciated area at the time of sedimentation.

There is a color change around 50 cm depth and a marked change in the number of foraminifera in the sediments. This might be connected to change in inflow of Atlantic surface water.

Diatoms found at 53-64 cm depth indicate changes in salinity and they do not occur under extensive sea ice cover.

References

Aagaard, K., and L.K. Coachman, 1968, The East Greenland Current north of Denmark Strait, Part I, *Arctic*, 21, 181-200

Benn and Evans, 2010, Glaciers and Glaciations. Hodder education. Second edition. Oxford U.K.

Dowdeswell, J.A., 1995. Glaciers in the High Arctic and recent environmental change. *Philosophical Transactions of The Royal Society*, Series A 352, 321–334

Hald, M., Korsun, S., 1997. Distribution of modern benthic foraminifera from fjords of Svalbard, *Journal of Foraminiferal Research*, 27, 101-122

Hald M., Steinsund P.I., Dokken T., Korsun S., Polyak L. & Aspeli R., 1994, Recent and late Quaternary distribution of Elphidium excavatumforma clavatain Arctic seas. *Cushman Foundation*, Special Publication no. 32, 141-153

Hansen A. & Knudsen K.L., 1995, Recent foraminiferal distribution in Freemansundet and Early Holocene stratigraphy on Edgeøya, Svalbard. *Polar Research*, 14, 215-238

Ingólfsson, Ó. & Hormes A., 2009, Guide to the Quaternary Geology of Western Svalbard, University Center in Svalbard. 9-10

Jakobsson, M, Løvlie, R, Arnold, E M, Backman, J, Polyak, L, Knutsen, J-O, and Musatov, E, 2001, Pleistocene stratigraphy and paleoenvironmental variation from Lomonosov Ridge sediments, central Arctic Ocean. *Global and Planetary Change*, 31, 1-22

Jessen S. P., Rasmussen T. L., Nielsen T., and Solheim A., 2010, A new Late Weichselian and Holocene marine chronology for the western Svalbard slope 30,000–0 cal years BP. *Quaternary Science Reviews*, 29, 1301-1312

Kjemperud, A., 1986, Late Weichselian and Holocene shoreline displacement in the Trondheimsfjord area, central Norway. Boreas 15, 61–82

Koc¸, N., D. Klitgaard-Kristensen, K. Hasle, C. F. Forsberg, and A. Solheim, 2002, Late glacial paleoceanography of Hinlopen Strait, northern Svalbard,Polar Res., 21, 307–314

Kubischta F., Knudsen K. L., Kaakinen A. & Salonen V., 2010, Late Quaternary foraminiferal record in Murchisonfjorden, Nordaustlandet, Svalbard. *Polar Research*, 287-290

Lyell, Charles, 1830, Principles of Geology.

Matthiessen, J, Niessen, F, Stein, R, and Naafs, B, 2010, Pleistocene glacial marine sedimentary environments at the eastern Mendeleev Ridge, Arctic Ocean, *Polarforschung*, 79, 123-137

Pinet, P.R., 2003. Invitation to Oceanography. 3rd Edition, Jones and Bartlett. (5th Edition, 2008) 92-97

Pirrung, M., Futterer, D., Grobe, J., Matthiessen, F., 2002. Magnetic susceptibility and ice-rafted debris in surface sediments of the Nordic Seas: implications for Isotope Stage 3 oscillations. *Geo-Marine letters* 22, 1-11

Rafferty J. P., 2011, Glaciers sea ice and ice formation. *Britannica educational publishing*, 164-165

Rogers K., 2011, Fungi, Algae, and Protists. *Britannica educational publishing*, 126-127

Rothwell, R. G. and Rack, F. R., 2006, New techniques in sediment core analysis: an introduction. Geological Society, London, *Special Publications*, 267, 1-29

Schlichtholz, P. and M.N. Houssais, 1999, An investigation of the dynamics of the East Greenland Current in Fram Strait based on a simple analytical model. *Journal of Physical Oceanography*, 29, 2240–2265

Ślubowska, M.A., Koç, N., Rasmussen, T.L., and Klitgaard-Kristensen, D., 2005, Changes in the flow of Atlantic water into the Arctic Ocean since the last deglaciation: Evidence from the northern Svalbard continental margin, 80°N. *Paleoceanography*, 20, 1-16

Ślubowska, M.A., Rasmussen, T.L., Koç, N., Klitgaard-Kristensen, D., Nilsen F., Solheim, A., 2007, Advection of Atlantic Water to the western and northern Svalbard shelf since 17,500 cal yr BP. *Quaternary Science Reviews*, 26, 463-478

Svendsen, J.I., Mangerud, J., 1997. Holocene glacial and climatic variations on Spits-bergen, Svalbard. *The Holocene* 7, 45-5

Stein, R., 2008, Arctic Ocean Sediments: Processes, Proxies and Paleoenvironment, 1st edition, *Elsevier Science*, 3-15, 177-181, 164-166,

Volkmann, R., 2000, Planktonic foraminifers in the outer Leptev Sea and the Fram Strait - modern distribution and ecology. *Journal of Foraminiferal Rescearch*, 30:3, 157-176

Wollenburg, J. E., Knies, J., & Mackensen, A., 2004, High-resolution paleoproductivity fluctuations during the past 24 kyr as indicated by benthic foraminifera in the marginal Arctic Ocean. *Paleogeography, Palaeoclimatology, palaeoecology. 204, 209-238*.

Zachos, J.C.; Pagani, M., Sloan, L., Thomas, E., and Billups, K., 2001), Trends, Rhythms, and Aberrations in Global Climate, 65 Ma to Present, *Science*, 292 (5517): 686–693

Appendix

Table 1 Magnetic Susceptibility

Position (cm)	Value 1	Value 2	Value average
2	89,2	125,9	107,55
4	56,4	31,6	44
6	37,2	33,8	35,5
8	34,4	44,6	39,5
10	23,4	19,3	21,35
12	30,4	28,4	29,4
14	23,2	18,9	21,05
16	22,4	17,8	20,1
18	22,6	18,2	20,4
20	22,9	18,4	20,65
22	22,8	18,3	20,55
24	23,9	19,7	21,8
26	24,2	19,8	22
28	24	20,3	22,15
30	23,9	20,7	22,3
32	27,6	24	25,8
34	25,9	23,8	24,85
36	31,8	28,2	30
38	37,7	33	35,35
40	38,4	34,4	36,4
42	43,1	40,2	41,65
44	42,7	39,9	41,3
46	44,3	41,1	42,7
48	43,4	38,9	41,15
50	39,5	36,4	37,95
52	36,8	36,8	36,8
54	36	34,2	35,1
56	34,6	31,9	33,25
58	33,1	30,9	32
60	39,1	37,2	38,15
62	47,1	42,9	45
64	39,7	37,7	38,7
66	39,3	39,8	39,55
68	43,1	42	42,55
70	42,5	40,5	41,5
72	40,1	38,2	39,15
74	39,6	38,2	38,9
76	37,3	35,7	36,5
78	37,5	36,2	36,85
80	41,2	36,1	38,65
82	31,6	30,4	31
84	34,3	31,1	32,7
86	32,5	31,9	32,2
88	39,5	38,5	39
90	43,3	42,3	42,8
92	41,1	39,2	40,15
94	40,5	39,6	40,05
96	43,7	42,1	42,9
98	46,3	46,3	46,3

Table 2 Shear Strength

Depth in core	cone	pen.avg	shear strength (kPa)
3	400g/30	4	175
6	100g/30	5	39
11	100g/30	9	15
16	100g/30	10,5	11
21	100g/30	9	15
26	100g/30	8	19
31	100g/30	8	19
36	100g/30	7	24
41	100g/30	6,5	27
46	100g/30	9,25	14
51	100g/30	9,5	13
56	100g/30	4,5	44
61	100g/30	6,5	27
66	100g/30	7	24
71	100g/30	5,75	32,5
76	100g/30	6,5	27
81	100g/30	5,5	34
86	100g/30	6,5	27
91	100g/30	7	24
96	100g/30	7,75	20

Table 3 Water Content

Depth		**Water content**					
depth [cm]	Sample no.	Weight cup [g]	Weight cup + wet sample [g]	Weight cup + dry sample [g]	Wet weight sample [g]	Dry weight sample [g]	Weigth % water content
2	1	3,38	9,307	8,0189	5,93	4,64	21,73
12	2	3,38	11,222	8,3924	7,84	5,01	36,08
22	3	3,38	10,616	7,7625	7,24	4,38	39,43
32	4	3,38	10,75	8,1268	7,37	4,75	35,59
42	5	3,38	10,476	8,0515	7,10	4,67	34,17
52	6	3,381	11,283	8,3166	7,90	4,94	37,54
62	7	3,381	12,023	8,9028	8,64	5,52	36,11
72	8	3,269	10,321	7,6743	7,05	4,41	37,53
83	9	3,731	11,9	8,9245	8,17	5,19	36,42
95	10	3,527	10,637	8,0338	7,11	4,51	36,61

Table 4 Granulometry

Grain-size distribution														
Weight cup (63 µm) [g]	Weight cup + sample (63 µm) [g]	Weight sample (63 µm) [g]	Weight cup (100 µm) [g]	Weight cup + sample (100 µm) [g]	Weight sample (100 µm) [g]	Weight cup (>1000 µm) [g]	Weight cup + sample (>1000 µm) [g]	Weight sample (>1000 µm) [g]		Weight % <63 µm	Weight % 63-100 µm	Weight % 100-1000 µm	Weight % > 1 mm	Sum (must be 100)
3,523	4,001	0,48	3,524	4,252	0,73	3,38	3,55	0,17		70,34	10,30	15,69	3,66	100,00
3,34	3,65	0,31	3,363	4,037	0,67	3,38	3,464	0,08		78,69	6,18	13,45	1,68	100,00
3,276	3,279	0,00	3,271	3,273	0,00	3,38	3,38	0,00		99,89	0,07	0,05	0,00	100,00
3,362	3,458	0,10	3,308	3,414	0,11	3,38	3,448	0,07		94,31	2,02	2,23	1,43	100,00
3,301	3,571	0,27	3,301	3,53	0,23	3,38	3,485	0,11		87,07	5,78	4,90	2,25	100,00
3,304	3,434	0,13	3,402	3,614	0,21	3,381	3,394	0,01		92,81	2,63	4,30	0,26	100,00
3,526	3,729	0,20	3,524	4,009	0,49	3,381	3,381	0,00		87,54	3,68	8,78	0,00	100,00
3,363	3,42	0,06	3,734	3,87	0,14	3,269	3,279	0,01		95,39	1,29	3,09	0,23	100,00
3,403	3,464	0,06	3,377	3,602	0,23	3,731	3,824	0,09		92,70	1,17	4,33	1,79	100,00
3,402	3,446	0,04	3,362	3,443	0,08	3,527	3,528	0,00		97,20	0,98	1,80	0,02	100,00

Table 5 Ice rafted debris per gram and foraminifers per gram

Sample no.	No. Squares Counted	No. Foram counted	No. IRD counted		No foram/g in sample	No of IRD/g in sample
1	45	5	34		1,077842	7,329324
2	45	82	37		16,35943	7,381693
3	45	1	0		0,22818	0
4	45	34	1		7,16272	0,210668
5	45	62	9		13,27197	1,926576
6	7	131	3		170,6262	0,607829
7	45	6	2		1,086602	0,362201
8	5	100	5		204,2994	1,134996
9	3	101	13		291,7108	2,503129
10	9	112	1		124,2567	0,221887

Table 6 Foraminifera Species Count

Forams							
Sample no.	Islandiella helenae	Cassidulina reniforme	Elphidium hallandense	Neogloboquadrina pachyderma	Stainforthia loeblichi	E. excavatum f. clavata	sum
1	4	1					5
2	11		7	64			82
3	1						1
4	9		3	22			34
5	29		4	28	1		62
6	24			105		2	131
7	0			6			6
8	44	1		55			100
9	3			98			101
10	39		1	72			112
%							
1	80,00%	20,00%					
2	13,41%		8,54%	78,05%			
3	100,00%						
4	26,47%		8,82%	64,71%			
5	46,77%		6,45%	45,16%	1,61%		
6	18,32%			80,15%		1,53%	
7	0,00%			100,00%			
8	44,00%			55,00%			
9	2,97%			97,03%			
10	34,82%		0,89%	64,29%			